Adaptive Covariance Tuning for Nonlinear Disturbance Force Estimation in Tethered Aerial Vehicles

Abdelateef NEGMELDEN[1], Nacim MESLEM[1], and Jonathan DUMON[1]

***Abstract*— Accurate force estimation is essential for robust control and improved model understanding in tethered aerial vehicles operating under uncertain wind conditions. These systems exhibit highly nonlinear and strongly coupled dynamics influenced by aerodynamic disturbances and tether forces. Extended Kalman Filters (EKF) are commonly used for joint state and disturbance estimation; however, their performance strongly depends on fixed process (Q) and measurement (R) noise covariance tuning.**

This paper proposes an adaptive covariance tuning strategy for unknown force estimation in tethered aerial systems modeled in spherical coordinates. Innovation- and residual-based statistics are used to update the Q and R matrices online. The approach is evaluated through simulation under multiple operating scenarios and validated using experimental flight data. Results show that selective covariance adaptation, particularly process noise adaptation, improves disturbance estimation accuracy while preserving filter stability.

***Index Terms*— Extended Kalman Filter, adaptive covariance tuning, unkown force estimation, nonlinear state estimation, tethered aerial vehicles**

I. INTRODUCTION

Renewable energy has become a central focus in modern energy systems due to environmental concerns and the limited availability of conventional fossil fuels [1]. Among renewable resources, wind energy plays a major role in global power generation. However, conventional wind turbines are constrained by tower height and structural limitations, with typical operating heights limited to about 150 m due to technological and structural constraints [2]. These limitations restrict their ability to fully exploit the available wind energy at higher altitudes.

Airborne Wind Energy (AWE) systems aim to overcome these constraints by harvesting wind energy at higher altitudes, where wind speeds are stronger and more consistent [3], [4], [7]. Unlike conventional turbines, AWE systems use tethered airborne platforms, such as flexible wings, rigid wings, or onboard generation systems, to access high-altitude winds [5]. During operation, aerodynamic lift generated by the airborne platform produces traction forces along the tether. These forces are transmitted to the ground unit and converted into electrical energy through a pumping cycle composed of a traction phase (reel-out) for power generation and a retraction phase (reel-in) for energy recovery [6], [7].

[1] Univ. Grenoble Alpes, CNRS, Grenoble INP, GIPSA-lab, 38000 Grenoble, France. Emails: abdelateef.khaled20@gmail.com, nacim.meslem@gipsa-lab.grenoble-inp.fr,jonathan.dumon@gipsa-lab.grenoble-inp.fr

Despite their strong potential, AWE systems face significant technical challenges due to highly nonlinear dynamics, strong tether coupling, and environmental disturbances arising from wind variability, aerodynamic uncertainties, and tether forces [8]. These effects become particularly critical during take-off, landing, and aggressive maneuvers, where neglected exogenous forces or poor disturbance compensation can severely degrade system stability and control performance [9].

In practice, the external aerodynamic and environmental forces acting on the aerial vehicle cannot be measured directly and must be estimated online [10]. Accurate disturbance force estimation is therefore essential to enhance robustness, improve control accuracy, and ensure safe and efficient operation under varying wind conditions.

Extended Kalman Filters (EKF) are widely adopted for nonlinear state and unknown estimation due to their computational efficiency and real-time applicability [11], [12]. In disturbance-augmented formulations, unknown external forces are modeled as additional states and estimated jointly with the system dynamics. However, the performance of the EKF strongly depends on the selection of the process noise covariance matrix Q and the measurement noise covariance matrix R [12]. In practice, these matrices are often tuned heuristically and kept fixed during operation. Such fixed covariance tuning may lead to degraded estimation accuracy when disturbance characteristics vary over time [13], particularly in nonlinear tethered systems operating under changing wind conditions.

This limitation motivates the development of adaptive force estimation strategies capable of updating the noise covariance matrices online to improve robustness and estimation accuracy under time-varying and uncertain operating conditions. Innovation- and residual-based covariance adaptation methods provide a practical framework for this purpose [14]. However, their impact on stability and estimation performance in nonlinear tethered aerial systems remains insufficiently investigated.

This paper proposes an innovation- and residual-based adaptive covariance tuning framework for unkown force estimation in tethered aerial vehicles modeled in spherical coordinates. The effects of adaptive process noise tuning and adaptive measurement noise tuning are systematically analyzed. Simulation studies under multiple operating scenarios, together with experimental validation using flight data, demonstrate that selective process noise adaptation improves disturbance estimation accuracy while preserving filter stability.

The remainder of the paper is organized as follows. Section II describes the system and its nonlinear model. Section III presents the baseline EKF formulation and the proposed adaptive covariance estimation method. Section IV provides simulation and experimental analysis. Finally, Section V concludes the paper.

II. NONLINEAR SYSTEM MODEL

This work considers a tethered airborne wind energy platform based on the Magnus-Based Winged Quadcopter (MWQ) system proposed in [15], as shown in Fig. 1. The vehicle is modeled in spherical coordinates aligned with the tether, providing a natural representation of the tethered configuration and explicitly capturing radial and angular motion. Aerodynamic, environmental, and winch-related effects are grouped as generalized disturbance forces.

A. System Dynamics

The augmented state vector includes the spherical position variables, their velocities, and unknown disturbance forces

$$x = \begin{bmatrix} r & \dot{r} & \eta & \dot{\eta} & \beta & \dot{\beta} & f_r & f_\eta & f_\beta \end{bmatrix}^T \in \mathbb{R}^9, \qquad (1)$$

where r denotes the tether length, η and β are the elevation and azimuth angles, and f_r, f_η, and f_β represent unknown forces acting along the tether-aligned spherical directions.

The control input vector is defined as

$$u = \begin{bmatrix} u_T & u_r & u_\eta & u_\beta \end{bmatrix}^T, \qquad (2)$$

where u_T is the winch control input, and u_r, u_η, and u_β denote the rotor thrust components expressed in the spherical coordinate frame.

The nonlinear dynamics are given by [15], [16]:

$$\frac{dr}{dt} = \dot{r}, \qquad \frac{d\eta}{dt} = \dot{\eta}, \qquad \frac{d\beta}{dt} = \dot{\beta} \qquad (3)$$

$$\begin{aligned} \frac{d\dot{r}}{dt} &= \frac{1}{m+m_w}\Big(mr\Omega + u_T - u_r - mg\sin\eta + f_r\Big), \\ \frac{d\dot{\eta}}{dt} &= \frac{1}{r}\Big(-2\dot{r}\dot{\eta} - r\dot{\beta}^2\cos\eta\sin\eta - g\cos\eta + \frac{u_\eta + f_\eta}{m}\Big), \\ \frac{d\dot{\beta}}{dt} &= \frac{1}{r\cos\eta}\Big(-2\dot{r}\dot{\beta}\cos\eta + 2r\dot{\beta}\dot{\eta}\sin\eta + \frac{u_\beta + f_\beta}{m}\Big). \end{aligned} \qquad (4)$$

where $\Omega = \dot{\eta}^2 + \dot{\beta}^2\cos^2\eta$.

The disturbance forces are assumed to be unknown and are modeled as additional state variables with zero dynamics:

$$\frac{df_r}{dt} = \frac{df_\eta}{dt} = \frac{df_\beta}{dt} = 0 \qquad (5)$$

The complete nonlinear system is written compactly as

$$\dot{x} = f(x,u). \qquad (6)$$

B. Measurement Equation

The available measurements consist of the spherical position components:

$$y = \begin{bmatrix} r & \eta & \beta \end{bmatrix}^T = h(x), \qquad (7)$$

with

$$h(x) = \begin{bmatrix} x_1 & x_3 & x_5 \end{bmatrix}^T. \qquad (8)$$

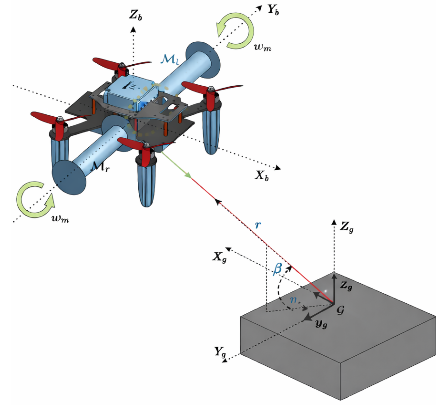

Fig. 1: Magnus-based winged quadcopter (MWQ) platform.

III. DISTURBANCE FORCE ESTIMATION

The nonlinear model described in Section II is used to estimate the unknown disturbance forces f_r, f_η, and f_β together with the system state vector. To achieve this objective, an Adaptative Extended Kalman Filter (EKF) is applied. This section first presents the baseline EKF formulation and then introduces the proposed adaptive covariance tuning strategy.

A. Baseline Extended Kalman Filter

The nonlinear system is expressed as

$$\dot{x}(t) = f(x(t), u(t)), \qquad z(t) = h(x(t)). \qquad (9)$$

To apply the EKF, the continuous-time model is discretized using a first-order Euler approximation with a sampling period T_s:

$$\begin{aligned} x_k &= f_d(x_{k-1}, u_{k-1}) + w_{k-1} \\ &= x_{k-1} + T_s f(x_{k-1}, u_{k-1}) + w_{k-1}, \\ z_k &= h(x_k) + v_k. \end{aligned} \qquad (10)$$

where $w_k \sim \mathcal{N}(0,Q)$ and $v_k \sim \mathcal{N}(0,R)$ denote the process noise and measurement noise, respectively [11].

Local linearization is performed using the Jacobian matrices

$$A_k = \left.\frac{\partial f_d}{\partial x}\right|_{\hat{x}^+_{k-1}, u_{k-1}}, \qquad H_k = \left.\frac{\partial h}{\partial x}\right|_{\hat{x}^-_k}. \qquad (11)$$

where $\hat{x}^+_{k-1}$ denotes the a posteriori state estimate at time $k-1$, and $\hat{x}^-_k$ denotes the a priori predicted state at time k.

EKF Algorithm

The filter is initialized with $\hat{x}_0$ and covariance P_0. The recursive estimation proceeds as follows [11].

Prediction step:

$$\hat{x}^-_k = f_d(\hat{x}^+_{k-1}, u_{k-1}), \qquad (12)$$

$$P^-_k = A_k P^+_{k-1} A^T_k + Q, \qquad (13)$$

Correction step:

$$K_k = P^-_k H^T_k \left(H_k P^-_k H^T_k + R\right)^{-1}, \qquad (14)$$

$$\hat{x}^+_k = \hat{x}^-_k + K_k\left(z_k - h(\hat{x}^-_k)\right), \qquad (15)$$

$$P^+_k = (I - K_k H_k) P^-_k. \qquad (16)$$

In the baseline implementation, the covariance matrices Q and R are selected heuristically based on physical insight into the system dynamics and sensor characteristics. The matrix Q is chosen diagonal, with smaller values assigned to position states, larger values to velocity states to account for modeling uncertainties, and higher values to disturbance force states representing unmodeled external effects. Similarly, R is selected according to sensor reliability, assigning smaller entries to low-noise measurements and larger values to noisier signals [15].

While this fixed tuning ensures stable performance under nominal conditions, it may lead to reduced estimation accuracy when disturbance and noise statistics vary over time. This limitation motivates the introduction of an adaptive covariance tuning strategy.

B. Adaptive Covariance Tuning Strategy

The proposed adaptive approach preserves the standard EKF prediction and correction structure presented previously. The state and covariance update equations remain unchanged; however, the covariance matrices Q and R are updated online using innovation- and residual-based statistics. This modification enables the filter to adapt to time-varying operating conditions while maintaining the original EKF framework [17], [18].

The innovation (d_k) and residual (ε_k) are defined as

$$d_k = z_k - h(\hat{x}_k^-), \qquad \varepsilon_k = z_k - h(\hat{x}_k^+). \tag{17}$$

These quantities provide complementary information regarding process and measurement uncertainties [17].

Residual-Based Adaptation of R_k

The measurement noise covariance matrix is updated using a residual-based covariance matching approach [18]:

$$R_k = \mathbb{E}\left[\varepsilon_{k-1}\varepsilon_{k-1}^T\right] + H_k P_k^- H_k^T. \tag{18}$$

To ensure numerical stability and smooth adaptation, an exponential forgetting factor $\alpha \in (0,1)$ is introduced:

$$R_k = \alpha R_{k-1} + (1-\alpha)\left(\varepsilon_{k-1}\varepsilon_{k-1}^T + H_k P_k^- H_k^T\right). \tag{19}$$

Innovation-Based Adaptation of Q_k

The process noise covariance matrix is adapted using the innovation sequence [17]. Since the innovation d_k is defined in the measurement space, it is projected into the state space through the Kalman gain. Using the same forgetting factor α, the recursive update is defined as

$$Q_k = \alpha Q_{k-1} + (1-\alpha) K_k d_k d_k^T K_k^T. \tag{20}$$

The forgetting factor α controls the trade-off between adaptation speed and stability. A large α gives smoother and more stable covariance updates but slower response to rapid disturbance changes, whereas a smaller α improves responsiveness but increases sensitivity to noise and transients. Thus, no fixed value is valid for all wind conditions or flight regimes. In this work, α was selected empirically to balance responsiveness and stability for the considered operating conditions.

Under this empirical tuning, the adaptive covariance updates allow the EKF to account for time-varying disturbances and modeling uncertainties while maintaining stable estimation behavior [17], [18].

IV. PERFORMANCE EVALUATION

The proposed estimation strategy is evaluated through both simulation-based and experimental studies.

Simulation-Based Evaluation

The following estimation configurations are considered:

- Baseline EKF with fixed covariance matrices.
- Adaptive process noise estimation (Q_k updated, R fixed) with two initialization strategies:
  - Model-based initialization.
  - Uniform (identity) initialization.
- Adaptive measurement noise estimation (R_k updated, Q fixed).

Each configuration is evaluated under multiple operating conditions. The estimated unknown forces are compared with ground-truth values, and estimation accuracy is quantified using the Root Mean Square (RMS) error.

Experimental Validation

The adaptive strategy is further validated using experimental flight data obtained under two control configurations:

- PID-Control configutation.
- SMC-Control configutation.

The adaptive Q_k and R_k approaches are compared with the baseline EKF to evaluate consistency and robustness under real operating conditions.

A. Simulation Results

The simulation study is conducted using a high-fidelity nonlinear model with , with access to ground-truth disturbance forces for quantitative accuracy assessment.

Baseline EKF

In the baseline configuration, the covariance matrices Q and R are fixed and selected heuristically. The process covariance is defined as

$$Q = \mathrm{diag}(10^{-10}, 20, 10^{-10}, 20, 10^{-10}, 20, 80, 80, 80), \tag{21}$$

with small weights on position states, moderate weights on velocity states, and larger weights on disturbance force states. The measurement covariance is chosen as

$$R = \mathrm{diag}(10^{-10}, 10^{-10}, 10^{-10}). \tag{22}$$

Zero-mean Gaussian noise is injected into the simulated measurements.

As shown in Fig. 2 the baseline EKF captures the dominant force trends in all spherical directions. However, transient deviations appear between 15 s and 25 s, mainly in the radial and azimuth components. These deviations increase the RMS error and indicate the sensitivity of fixed covariance tuning to time-varying disturbance dynamics.

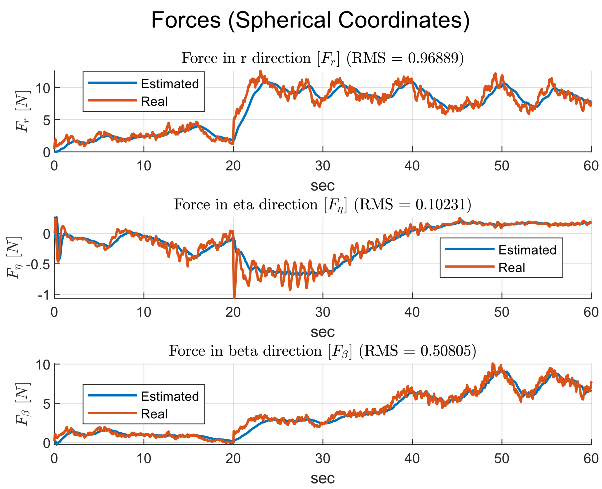

Fig. 2: Force estimation using the baseline EKF.

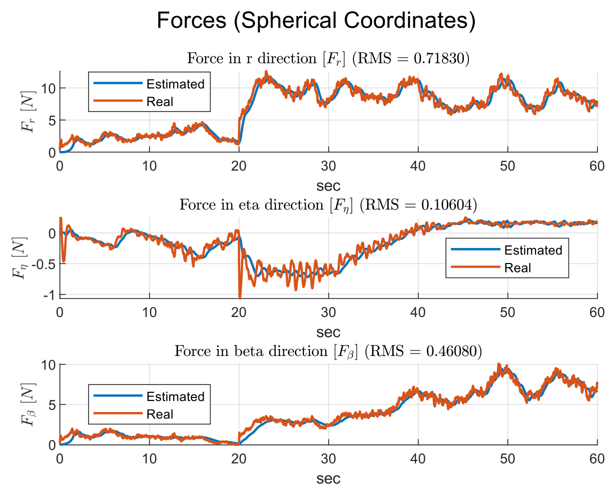

Fig. 4: Force estimation using adaptive process noise covariance Q_k with identity initialization.

Adaptive Process Noise Estimation (Q_k Adaptive)

In this configuration, the process covariance Q_k is updated online while R remains fixed. Two initialization strategies are considered to evaluate the influence of the initial covariance selection on estimation performance.

1) Model-Based Initialization: Q_k is initialized using the nominal diagonal values of the baseline EKF.

2) Identity Initialization: Q_k is initialized as an identity matrix $Q_k(0) = \mathrm{diag}(1, 1, 1, 1, 1, 1, 1, 1, 1)$.

As shown in Figs. 3 and 4, adaptive process noise estimation improves unknown force tracking compared with the baseline EKF, particularly in the radial and azimuth components, where lower RMS errors are observed.

The model-based initialization (Fig. 3) gives slightly lower RMS errors than identity initialization (Fig. 4), indicating faster convergence with physically informed covariance values. However, identity initialization still outperforms the baseline EKF, confirming the effectiveness of adaptive process noise estimation without prior covariance information.

To further examine the adaptation behavior, Fig. 9 shows the eigenvalues of Q_k under identity initialization. Starting from equal covariance weights, adaptive Q_k reshapes the covariance structure according to the system dynamics. Relatively, the position directions (λ_1–λ_3) keep the lowest weights, the velocity directions (λ_4–λ_6) take intermediate weights, and the disturbance-force directions (λ_7–λ_9) receive the highest weights. This relative separation indicates a physically consistent covariance structure despite the non-informative initialization.

Adaptive Measurement Noise Estimation (R_k Adaptive)

In this configuration, the measurement covariance R_k is updated online while Q remains fixed at the nominal diagonal values of the baseline EKF.

As shown in Fig. 5, the estimated disturbance forces follow the ground-truth values across the simulation. However, the RMS error reduction remains limited and close to the baseline EKF, indicating that adaptive measurement noise tuning is less effective in capturing time-varying disturbance dynamics.

Performance Validation Across Different Scenarios

For robustness assessment of the proposed estimation approaches, all introduced configurations are evaluated across three distinct simulation scenarios.

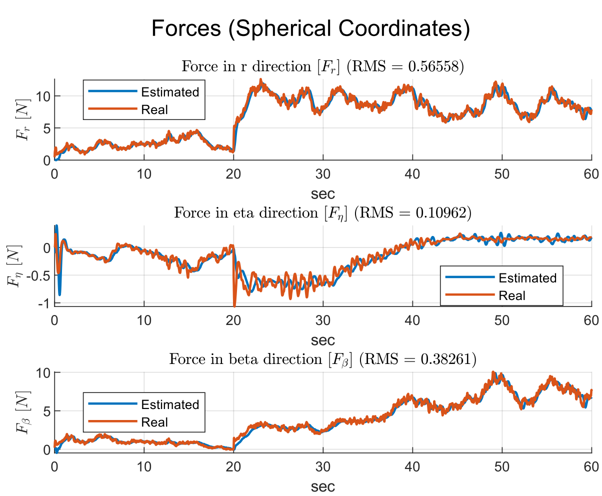

Fig. 3: Force estimation using adaptive process noise covariance Q_k with model-based initialization.

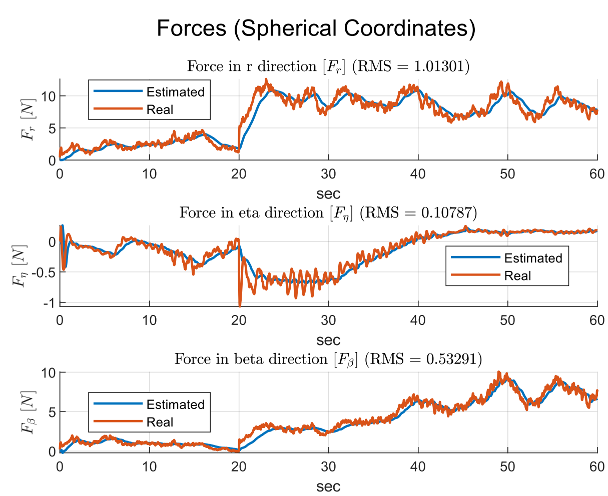

Fig. 5: Force estimation using adaptive measurement noise covariance R_k.

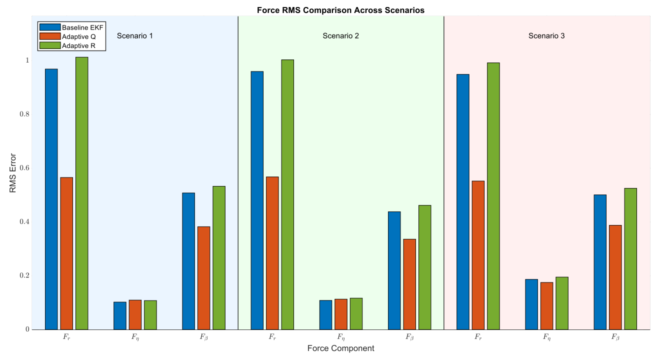

Fig. 6: RMS force estimation errors of baseline EKF, adaptive Q_k, and adaptive R_k across scenarios.

- Scenario 1: Nominal reference inputs.
- Scenario 2: Increased radial reference excitation.
- Scenario 3: Increased azimuth reference excitation.

For each scenario, disturbance forces are estimated and the Root Mean Square (RMS) errors are computed to compare performance across methods.

As shown in Fig. 6, the adaptive Q_k approach achieves the lowest RMS errors across the three scenarios, especially for the radial (f_r) and azimuth (f_β) force components. In contrast, the baseline EKF and adaptive R_k give comparable results, with higher errors than adaptive Q_k.

This improvement is mainly due to the dominant uncertainty being related to the model dynamics, especially the zero-dynamics assumption made for the unknown force states. In the augmented EKF, the forces f_r, f_η, and f_β are assumed constant, whereas in practice they vary due to wind, tether motion, aerodynamic effects, and control actions. Thus, the main mismatch is related to the process model rather than measurement noise. Adapting Q_k directly accounts for this imperfect force-dynamics model, while adapting R_k only changes the confidence assigned to the measured variables r, η, and β, explaining the better effect of adaptive process-noise tuning on force-estimation accuracy.

Simultaneous adaptation of Q_k and R_k was also tested, but led to divergence under sudden measurement changes. Since both updates rely on the innovation and residual computed from the same measurement z_k, a sudden change can be interpreted simultaneously as process and measurement uncertainty. This creates conflicting effects on the Kalman gain, producing inconsistent covariance updates and loss of filter stability.

B. Experimental Validation

The proposed estimation strategies are further evaluated using experimental flight data collected under PID and SMC control configurations. The experimental data used in this study are available in the following deposit [19]. The reference inputs are fixed at $r_d = 20$ m, $\eta_d = 0°$, and $\beta_d = 45°$.

Since ground-truth disturbance forces are not available in the experimental data, direct RMS force errors cannot be computed. Therefore, the experimental validation is based on a qualitative comparison between the baseline EKF and the adaptive estimators. The winch tension is also included

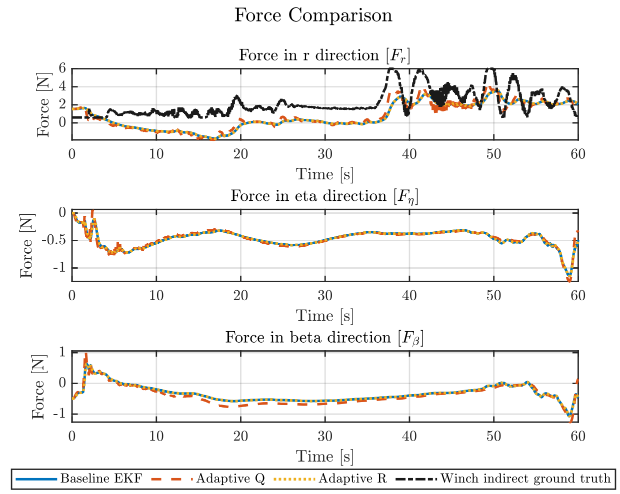

Fig. 7: Experimental force estimation under PID control configuration.

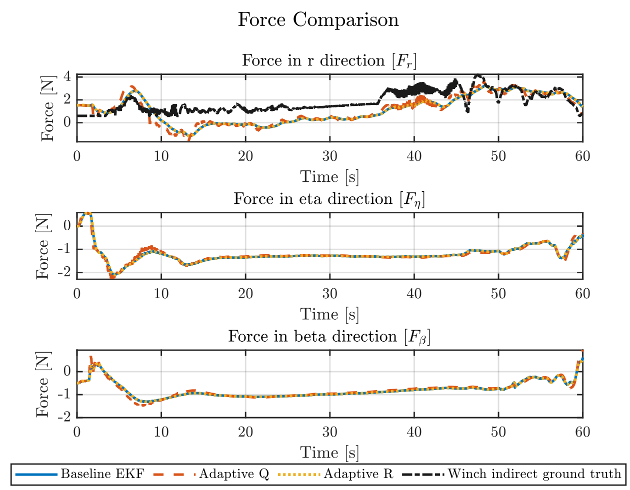

Fig. 8: Experimental force estimation under SMC control configuration.

as an indirect reference for the radial force trend, since it is physically related to the tether-direction dynamics. This choice is motivated by observations in simulation, where we found that the ground-truth radial force and the winch input follow similar dynamic trends, with different amplitudes. Thus, the winch tension is not considered as an exact ground truth, but only as a supporting reference for interpreting the radial force behavior.

As shown in Figs. 7 and 8, the three estimators exhibit similar overall force trends under both control configurations. The adaptive R_k estimator remains close to the baseline EKF, which is consistent with the simulation results and indicates the limited effect of measurement-noise adaptation. In contrast, the adaptive Q_k estimator shows more noticeable variations, especially in the radial (f_r) and azimuth (f_β) components, where the simulation results also showed the largest improvement.

For the radial component, the adaptive Q_k estimate follows the main trend of the winch tension more clearly than the adaptive R_k estimate. This supports the qualitative interpretation that adaptive process-noise tuning is more responsive to radial force dynamics. Since the winch tension is only an indirect reference, this comparison is used to assess trend consistency rather than exact force-estimation accuracy.

Overall, the experimental results follow the same trend observed in simulation: adaptive R_k remains close to the baseline EKF, while adaptive Q_k is more responsive to time-varying force dynamics. These results provide qualitative and indirect validation in the absence of ground-truth disturbance-force measurements.

V. CONCLUSIONS

This paper investigated disturbance force estimation for a tethered aerial vehicle using a disturbance-augmented EKF formulated in spherical coordinates. Innovation- and residual-based covariance updates were introduced to adapt Q_k and R_k online while preserving the standard EKF structure.

Simulation results across three excitation scenarios show that adapting the process covariance Q_k provides the largest reduction in force estimation error, particularly for the radial (f_r) and azimuth (f_β) components. Model-based initialization improves convergence, while identity initialization still recovers a consistent covariance structure after a transient.

Adapting only the measurement covariance R_k yields performance close to the baseline EKF while eliminating manual tuning. In contrast, simultaneous adaptation of Q_k and R_k leads to divergence under the considered sensing configuration, indicating coupling effects between the covariance updates.

Experimental flight data under PID and SMC control scheme the same trend observed in simulation: adaptive R_k remains close to the baseline EKF, whereas adaptive Q_k introduces systematic estimation variations, supporting the benefit of process noise adaptation for disturbance estimation.

APPENDIX

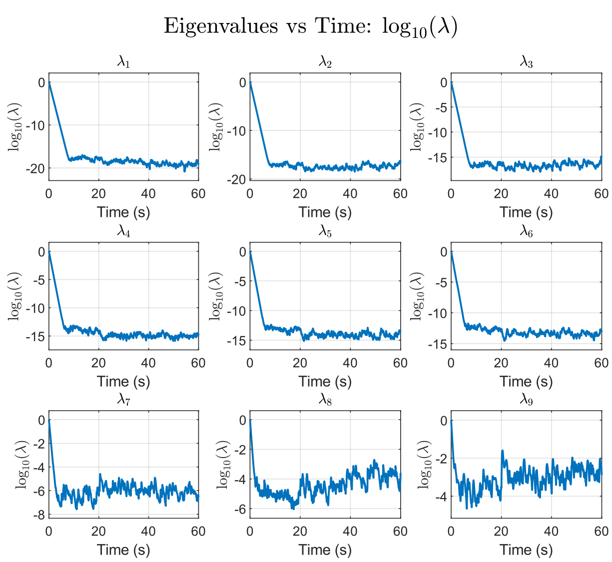

Fig. 9: Time evolution of the eigenvalues of the adaptive process noise covariance matrix Q_k under identity initialization.

ACKNOWLEDGMENT

This work has been partially supported by ROBOTEX 2.0 through the grants ROBOTEX ANR-10-EQPX-44-01 and TIRREX ANR-21-ESRE-0015, funded by the French program *Investissements d'avenir*. The authors also thank Amaury Negre, Alexis Offermann, Pierre Susbielle and Zakeye Azaki for the development of the experimental platform and simulation framework that enabled this work.

REFERENCES

[1] United Nations, "Renewable energy – Raising ambition," United Nations Climate Action, [Online]. Available: https://www.un.org/en/climatechange/raising-ambition/renewable-energy.

[2] L. Fagiano, M. Milanese, and D. Piga, "High–altitude wind power generation," Technical Report DAUIN TR FaMiPi 27082009, Politecnico di Torino, Italy, 2009.

[3] P. Bechtle, M. Schelbergen, R. Schmehl, U. Zillmann, and S. Watson, "Airborne wind energy resource analysis," *Renewable Energy*, vol. 141, pp. 1103–1116, 2019,

[4] M. L. Loyd, "Crosswind kite power," *Journal of Energy*, vol. 4, no. 3, pp. 106–111, 1980.

[5] A. Cherubini, A. Papini, R. Vertechy, and M. Fontana, "Airborne wind energy systems: A review of the technologies," *Renewable and Sustainable Energy Reviews*, vol. 51, pp. 1461–1476, 2015.

[6] L. Fagiano and M. Milanese, "Airborne wind energy: An overview," *IEEE Control Systems Magazine*, vol. 32, no. 6, pp. 46–65, 2012.

[7] L. Fagiano, M. Milanese, and D. Piga, "Autonomous airborne wind energy systems: accomplishments and challenges," *Annual Review of Control, Robotics, and Autonomous Systems*, vol. 5, no. 1, pp. 603–631, 2022.

[8] M. Diehl, R. Schmehl, and U. Ahrens, "Airborne wind energy: Basic concepts and physical foundations," in *Airborne Wind Energy*, Springer, 2013, pp. 3–22.

[9] A. Schanen, J. Dumon, N. Meslem, and A. Hably, "Take-off and landing of an AWE system using a multicopter," in *Proc. American Control Conference (ACC)*, Denver, CO, USA, Jul. 2020,

[10] Z. Ahmed and C. A. Woolsey, "An invariant extended Kalman filter for wind estimation using a small, fixed-wing uncrewed aerial vehicle," *IEEE Transactions on Control Systems Technology*, vol. 33, no. 5, pp. 1799–1809, Sep. 2025,

[11] G. Welch and G. Bishop, "An Introduction to the Kalman Filter," Univ. North Carolina at Chapel Hill, Tech. Rep., 2006.

[12] D. Simon, *Optimal State Estimation*. Hoboken, NJ, USA: Wiley, 2006.

[13] Y. Huang, Y. Zhang, Z. Wu, N. Li, and J. Chambers, "A novel adaptive Kalman filter with inaccurate process and measurement noise covariance matrices," *IEEE Transactions on Automatic Control*, vol. 63, no. 2, pp. 594–601, Feb. 2018,

[14] S. Akhlaghi, N. Zhou, and Z. Huang, "Adaptive adjustment of noise covariance in Kalman filter," *arXiv preprint arXiv:1702.00884*, 2017.

[15] A. Azaki, "Autonomous magnus-based winged quadcopter system for prolonged flight and tethered airborne wind energy applications," Ph.D. dissertation, Université Grenoble Alpes, Grenoble, France, 2024.

[16] Z. Azaki, J. Dumon, N. Meslem, A. Hably, and P. Susbielle, "Modelling and control of a tethered drone for an AWE application," in *Proc. 6th Int. Conf. on Control, Automation and Diagnosis (ICCAD)*, Lisbon, Portugal, Jul. 2022, pp. 1–6,

[17] S. Akhlaghi, N. Zhou, and Z. Huang, "Adaptive adjustment of noise covariance in Kalman filter for dynamic state estimation," *IEEE Transactions on Control Systems Technology*, vol. 30, no. 3, pp. 1048–1060, 2022,

[18] Y.-W. Chen and K.-M. Tu, "Robust self-adaptive Kalman filter with application in target tracking," *Measurement and Control*, vol. 55, no. 9–10, pp. 935–944, 2022,

[19] Z. Azaki, J. Dumon, A. Offermann, P. Susbielle, A. Negre, N. Meslem, and A. Hably, "Indoor and Outdoor flights for Tethered Magnus-effect Winged Quadcopter System Under Wind Disturbance," Recherche Data Gouv, Dataset, Version V1, 2026, doi: 10.57745/MVGMUH.